View metadata, citation and similar papers at core.ac.uk

brought to you by CORE

provided by Open Archive Toulouse Archive Ouverte

Sliding lubricated anisotropic rough surfaces

F. Plouraboué, M. Prat, and N. Letalleur

Institut de Mécanique des Fluides de Toulouse, UMR CNRS-INP/UPS No.5502, Avenue du Professeur Camille Soula, 31400 Toulouse, France

The object of this paper is to study the effects of lubricant film flow, pressurized and sheared between two parallel rough surfaces in sliding motion. The influence of microscopic surface roughness on lubricant film flow macroscopic behavior is described through five nondimensional parameters called flow factors. These macroscopic transport parameters are related to the local geometry of apertures and surfaces. Short- and long-range-correlated surface roughnesses display very different macroscopic behaviors when surfaces are close to contact. These behaviors are related to underlying surface roughness parameters such as the correlation length and the self-affine Hurst exponent. The problem is numerically studied, and results are compared to some analytical asymptotic results.

I. INTRODUCTION

A problem consisting of lubricating two sliding surfaces is encountered in many mechanical and tribological applications. When sliding surfaces become close, the lubricant motion becomes increasingly dependent on the surface topography. This can be the case in the context of reading and recording devices such as magnetic recording disks [1], or rolling processes [2]. In those applications it may be crucial to estimate the lubricant interaction with solid surfaces in order to prevent contact between two solids which could damage the surfaces. Hence many authors have devoted time and effort to elaborate models in order to estimate this small scale interactions between surfaces and lubricant [3,4].

On the other hand, surface topography itself has received great attention in many areas due to the growing development of refined measurements using mechanical, optical, or electrical probes. In the context of engineering surfaces, many studies were devoted to surface topography measurements [5], showing in many cases multiscale surface roughness. This has been shown in the case of forming or finishing processes (shaping and lapping, [6]) electrodischarge machining, [7] sand blasting, [8] or rolling [9]. In the case of magnetic recording disks [10,11] or rolled sheets [12] surfaces have been shown to be anisotropic and self-affine. An abundant literature (see Ref. [13], and references therein) shows increasing evidence that industrial machined surfaces display long-range correlated surface roughness at a small scales.

Hence it seems natural to address the question of what influence such geometrical properties may have on fluid-solid interactions at a macroscopic scale. Such a question has received considerable attention in different contexts, among them the transport properties of fractures [14]. The influence of self-affine fracture roughness on some geometrical properties [15,16], on electrical conductance and permeability, [17–20], on macro dispersion [21], on percolation [22,23], and on drainage [24] has already been investigated.

As for sliding surfaces, short-range roughness geometry has been studied by many authors (see Ref. [4]). This study investigates a comparison between short- and long-range correlated geometries on macroscopic transport coefficients of lubricated sliding surfaces. The paper is organized as follows. In Sec. II we introduce the considered geometry, and recall the results of macroscopization of the Reynolds equation. We introduce macroscopic transport coefficients called flow factors, which describe the influence of roughness at the macroscale. Section III presents the flow factors obtained for two independent sliding surfaces admitting short- and long-range correlations. Two particular asymptotic regimes are discussed, when surfaces are far from each other or, conversely, close to contact. In the latter case, the flow factor dependence on the correlation length or the Hurst exponent has been explicitly obtained.

II. FROM MICROGEOMETRY TO MACROSCOPIC FLOW SCALE

A. Surface geometry

This study considers random surfaces, for which the scale of the ''macroscopic'' geometry and the ''microscopic'' roughness are greatly distinct. This configuration is found in many situations for which, for example, a submillimeter roughness is superposed on that of some centimeter scale surfaces variations, as encountered in Ref. [12]. Moreover, this work focuses on the case where the microscopic structure is invariant along one direction. The macroscale surface is thus defined by a single valued function $Z(X,Y)$—we capitalize when referring to the macrostructure — while the microscale has a one-dimensional roughness $z(x)$ along the x axis. The variables X and Y vary very slowly in space compared to x, so that the typical X and Y length-scale variations are considered to be large in comparison to the x variation, which is usually called the elementary representative scale, and will be referred to as L.

Such surfaces are encountered in various contexts such as magnetic recording disks [10,11] or rolled surfaces [12]. An example of microscale anisotropic surface topography is represented in Fig. 1, obtained from an atomic force microscopy measurement in Ref. [12]. In the following, we will focus on the statistical property of the microscopic surface height correlation function $C(u)$,

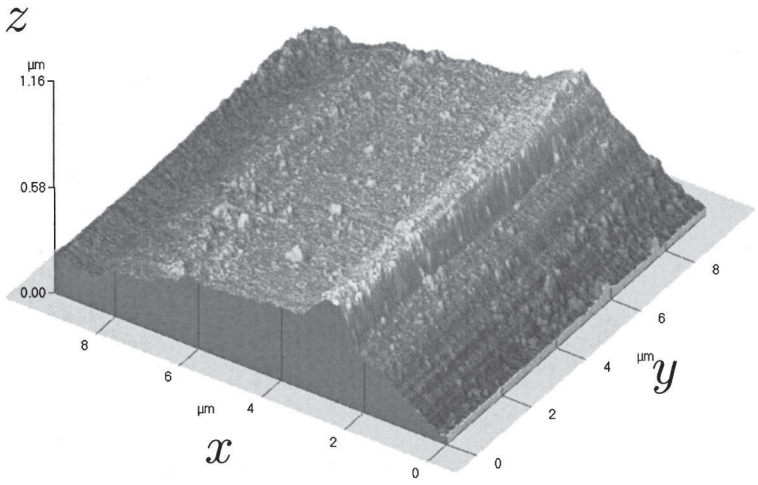

FIG. 1. An example of a microscopic view of an anisotropic surface topography from Ref. [12], using an atomic force microscope

$$C(u)=\langle[z(x)-z(x+u)]^2\rangle, \tag{1}$$

where the average $\langle\cdots\rangle$ is taken over x, along the representative typical scale L. Short-range-correlated surfaces exhibit a correlation length λ, such that $C(u,\lambda)=C(u/\lambda)$, for which $C(u/\lambda)$ becomes constant when $u\gg\lambda$. The exact correlation function expression is generally not significant in comparison to the precise value of the correlation length λ.

Long-range-correlated surfaces display different properties. As previously mentioned, fractional Brownian motion (fBm) is a rather good description of many long-range-correlated manmade surfaces. These self-affine profiles have the interesting property of being statistically invariant through the affine transformation $x\to\alpha^{1/\zeta}x$. Hence the correlation function satisfies $C(\alpha u)=\alpha^{2\zeta}C(u)$ for positive α, or

$$C(u)=C(\ell_c)\left|\frac{u}{\ell_c}\right|^{2\zeta}, \tag{2}$$

where ζ is called the roughness or Hurst exponent, and ℓ_c is an arbitrary microscopic length scale, the lower cutoff. This length has been shown to be a few tens of nanometers for the surface represented in Fig. 1. Scaling (2) permits an easy measurement of the Hurst exponent from the computation of the height power spectrum $P(k)=|\tilde{z}(k)|^2\propto k^{-1-2\zeta}$, which is the square of the Fourier transform of the profile height. It displays a well-defined power law of the wave vector k. An example of such a spectrum, obtained from different measurements on rolled surfaces [12], is shown in Fig. 2. It displays three decades of self-affine roughness, from a few tens of nanometers to a few tens of microns. Expanding the expression of $C(u)$ in Eq. (1) leads to an equivalent form:

$$\frac{\langle(z(x)-Z)(z(x+u)-Z)\rangle}{\langle(z(x)-Z)^2\rangle}=1-A^2\left(\frac{u}{\ell_c}\right)^{2\zeta}, \tag{3}$$

where the macroscale surface height Z is the mean of the microscale surface height $Z=\langle z\rangle$, and

$$A^2=\frac{C(\ell_c)}{2\langle[z(x)-Z]^2\rangle}. \tag{4}$$

A is a characteristic parameter of the surface, usually called the roughness amplitude. The roughness amplitude of self-affine surfaces can also be described by another parameter called the topothesy t, which is the characteristic scale for which local roughness slopes are of order 1. As a matter of fact, the slopes of self-affine surfaces increase as the observation scale decreases. The topothesy is interesting to consider because the Reynolds approximation used below is only valid for surfaces with small slopes. Thus the Reynolds approximation can adequately describe the flow field at a scale much larger than t. For example, the topothesy t was evaluated in Ref. [12] to be of the order of ten nanometers for rolled surfaces. In the following, we will consider both short- and long-range-correlated profiles at the microscale.

B. Kinematics and microscopic flow

Two sliding surfaces lubricated by a Newtonian fluid are considered. The macroscopic geometry, sketched in Fig. 3, shows that, at the macroscopic scale, the aperture H between top and bottom surfaces $H(X,Y)=Z_2(X,Y)-Z_1(X,Y)$ can be fully two dimensional. The top surface, number 2, slides with velocity $\mathbf{U}_2$ not necessarily collinearly with that of the lower surface 1, $\mathbf{U}_1$. The mean planes of the surfaces are

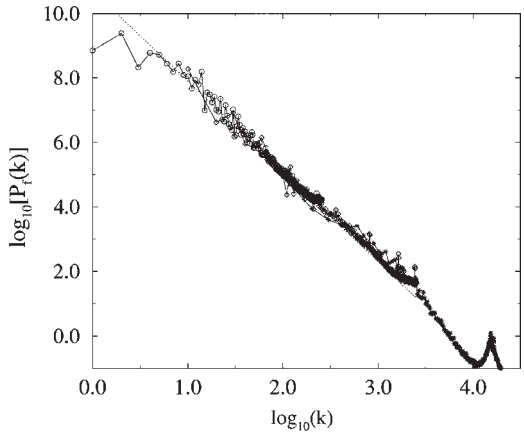

FIG. 2. Power spectra of the laminated surface profile obtained in Ref. [12].

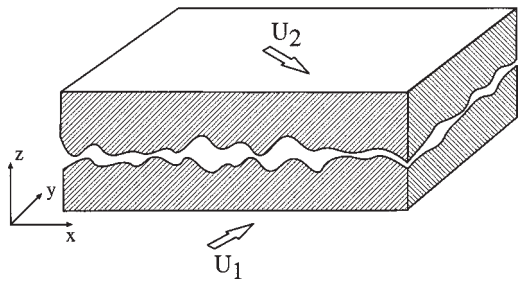

FIG. 3. System of two rough surfaces in sliding motion: a macroscopic view.

considered to be parallel. A reference plane $z=0$ is introduced, and each surface is described by its local height z_i, with macroscopic height $\langle z_i \rangle = Z_i$, where $i=1$ and 2. In this study it will be considered that both surface roughness are independent, and that deformations of surfaces are ignored. Contacts between surfaces are not permitted. Hence the local aperture, defined by $a=z_2-z_1$ is always positive. The mean local aperture $\langle a \rangle$ at the microscale is simply related to the local macroaperture H, $\langle a \rangle = H = Z_2 - Z_1$.

In such a confined geometry, inertial effects are generally negligible, associated with a very small Reynolds number. The laminar fluid flow between two rough surfaces is generally simply not related to the surface topography [25]. An important exception occurs when surface slopes are small everywhere. In this context, which covers a broad range of manmade surfaces, the Stokes formulation of the momentum equation is simplified by the Reynolds (lubrication) approximation. In this approximation the pressure is constant over the local aperture between the solid surfaces, and the local velocity field has a negligible vertical component. The velocity field has two contributions: a Couette one coming from flow due to moving boundaries, and a Poiseuille one coming from the pressure gradient. The Couette contribution admits a local linear vertical dependence, while the Poiseuille one has a vertical parabolic profile. The pressure field completely determines the flow field, and is related to the geometry by a bidimensional local Reynolds equation,

$$\nabla \cdot \left(\frac{a^3}{12\mu} \nabla p \right) = \frac{1}{2} \nabla a \cdot (\mathbf{U}_2 + \mathbf{U}_1), \tag{5}$$

where p denotes the pressure at the microscale, and μ is the lubricant viscosity. The Reynolds equation is thus similar to a heterogeneous Darcy law with a permeability $a^3/12$ related to the underlying local distance between surfaces. The surface velocities act as a source term that will locally increase the flow, and thus the pressure. When the local microscopic scale is very small compared to the large scale macroscopic description, one may find a homogenized macroscopic equation for the local Reynolds equation (5).

C. Macroscopic Scale

By using homogeneization or volume averaging techniques as shown in Refs. [26–28], one can relate the spatially averaged divergence free unit flow $\mathbf{Q}$ to the macroscopic pressure P through the equation

$$\mathbf{Q} = -\frac{H^3}{12\mu} \boldsymbol{\phi} \cdot \nabla P + \frac{H}{2} (\mathbf{U}_2 + \mathbf{U}_1) + \frac{\sigma}{2} \boldsymbol{\phi}_s \cdot (\mathbf{U}_1 - \mathbf{U}_2), \tag{6}$$

where σ is the composite root mean square (rms) roughness classically defined as $\sigma = \sqrt{\sigma_1^2 + \sigma_2^2}$ (where $\sigma_i = \sqrt{(z_i - Z_i)^2}$ is the rms microscopic roughness of surface i). Reynolds flow factor $\boldsymbol{\phi}$ and $\boldsymbol{\phi}_s$ are diagonal tensors in the (x,y) coordinate frame given by

$$\boldsymbol{\phi} = \begin{pmatrix} \phi_x & 0 \\ 0 & \phi_y \end{pmatrix} = \begin{pmatrix} \dfrac{1}{H^3 \langle a^{-3} \rangle} & 0 \\ 0 & \dfrac{\langle a^3 \rangle}{H^3} \end{pmatrix}$$

$$\boldsymbol{\phi}_s = \begin{pmatrix} \phi_s = \dfrac{1}{\sigma \langle a^{-}3 \rangle} \left\langle \dfrac{z_1 - Z_1 + z_2 - Z_2}{a^3} \right\rangle H & 0 \\ 0 & 0 \end{pmatrix}. \tag{7}$$

The left term $\boldsymbol{\phi}$ is nothing but a reformulation of the well-known composition of parallel or series resistances, and is related to pressure forcing. The ϕ_y parameter, associated with parallel resistances, will not be analyzed further in the following because of its trivial dependence on the aperture field, i.e, the third moment of the aperture distribution, which does not depend on the two point correlation of the aperture. Conversely, the first flow factor ϕ_x does depend on this correlation structure, and thus will be of interest in the following sections. The second tensor $\boldsymbol{\phi}_s$, which has only one nonzero component, comes from the mean contribution of the surface motion on the lubricant flux, in the roughness streak direction. Similarly the tangential shear vector $\boldsymbol{\tau}$, which is the stress tensor projection tangentially to the mean surface plane, can be homogenized and exhibits some Couette and Poiseuille contributions,

$$\boldsymbol{\tau}_{\pm} = \frac{\mu}{2} (\phi_f \boldsymbol{I} \pm \boldsymbol{\phi}_{fs}) \cdot (\mathbf{U}_2 - \mathbf{U}_1) \pm \frac{H}{2} \boldsymbol{\phi}_{fp} \cdot \nabla P, \tag{8}$$

where $\boldsymbol{\tau}_+$ is associated with the upper surface, $\boldsymbol{\tau}_-$ with the lower one, and $\boldsymbol{I}$ is the identity tensor. The Couette shear flow factors tensors are again diagonal in the (x,y) frame, and read

$$\phi_f = H \langle a^{-1} \rangle$$

$$\boldsymbol{\phi}_{fs} = \begin{pmatrix} \phi_{fs} = 3H \left[\left\langle \dfrac{z_1 + z_2 - Z_1 - Z_2}{a^3} \right\rangle \dfrac{\langle a^{-2} \rangle}{\langle a^{-3} \rangle} - \left\langle \dfrac{z_1 + z_2 - Z_1 - Z_2}{a^2} \right\rangle \right] & 0 \\ 0 & 0 \end{pmatrix}. \tag{9}$$

The first term is scalar, and comes from the average of the Couette shear of sliding surfaces. The second term is less intuitive, and shows some dependence on both the surface

height and the local aperture. The Poiseuille shear flow factor, driven by the pressure gradient, reads

$$\boldsymbol{\phi}_{fp}=\begin{pmatrix}\phi_{fp} & 0\\ 0 & \dfrac{\langle a\rangle}{H}\end{pmatrix}=\begin{pmatrix}\dfrac{\langle a^{-2}\rangle}{H\langle a^{-3}\rangle} & 0\\ 0 & \dfrac{\langle a\rangle}{H}=1\end{pmatrix}. \quad (10)$$

Hence macroscopic effective equations can be explicitly related to the microstructure geometry, i.e, to the local aperture and surface height, through five nondimensional parameters. Two of these are associated with the pressure gradient and are called Poiseuille flow factors (i.e., ϕ_x,ϕ_{fp}). Three of them are associated with the surface relative velocity, and are thus called Couette flow factors (i.e., ϕ_s,ϕ_f,ϕ_{fs}). In the special case considered here, surfaces 1 and 2 are uncorrelated. The aperture field can be considered to be decomposed of two surfaces of heights equal to zero and z_2-z_1 [29]. Then it can be deduced that the Couette flow factors depend only on the local aperture field, through

$$\phi_s=\frac{\sigma_1^2-\sigma_2^2}{\sigma^2}\Phi_s(H,\sigma,\{a\}),\quad \phi_{fs}=\frac{\sigma_1^2-\sigma_2^2}{\sigma^2}\Phi_{fs}(H,\{a\}) \quad (11)$$

where σ is the composite roughness and

$$\Phi_s=\frac{1}{\sigma}\left(H-\frac{\langle a^{-2}\rangle}{\langle a^{-3}\rangle}\right)\quad \Phi_{fs}=3H\left(\langle a^{-1}\rangle-\frac{\langle a^{-2}\rangle^2}{\langle a^{-3}\rangle}\right). \quad (12)$$

It is noteworthy that in the case where both independent surfaces share the same rms roughness, flow factors ϕ_s and ϕ_{fs} cancel out. This is a manifestation of the statistical symmetry of the surfaces, which is also recovered for deterministic symmetrical surfaces. Section III studies how these surfaces vary with the macroscopic aperture H and the microgeometry statistical properties. In the following, it is considered that the height distribution of each surface results from a Gaussian stochastic process. Being the difference between two Gaussian processes, the aperture field is also a Gaussian process, and therefore is fully characterized by its mean and covariance. It is thus investigated how the aperture correlation influences the transport properties of the lubricant between the two sliding surfaces, through flow factors.

III. FLOW FACTOR COMPUTATION

From definitions (7)–(12), it is now possible to compute flow factors. Nevertheless, their average on stochastic microgeometries are mainly the quantities of physical interest. Such a statistical description needs to perform its average on the random surface height. This computation is numerically performed, and compared to analytical estimates.

The numerically generated profile correlation function can be prescribed using their Fourier formulation [30]. A Hermitic representation $\tilde{z}(k)=-\tilde{z}^{\star}(-k)$ imposes a real profile. Gaussian height probability distributions of profile are obtained from complex Gaussian amplitudes of the height Fourier representation. The chosen wave vector dependence of the height Fourier transform allows one to generate either a short-range-correlated height profile or fractional Brownian motion.

The flow-factor computation has been achieved with an exact integration scheme. Generically, one only needs to spatially integrate some integer power of the local aperture a^n, for which an exact expression of the integration elements is easy to perform. When surfaces are close to contact, this precise procedure avoids using an adaptative step integration, and minimizes the computation error. The profile length L and the number of profiles have been varied so that the computed quantities satisfactorily reach their mean estimate. Typically, L has been chosen between 512 and 2048, and the number of realizations from 500 to 1000.

A. Short-range correlated Gaussian surfaces

This section considers finite correlated microgeometry profiles. The correlation length is bounded by the composite roughness σ and the elementary representative scale L, i.e, $\sigma<\lambda<L$. The first bound, σ, is related to the small slope hypothesis that underlies a flow-factor macroscopic description through the lubrification approximation. The second bound comes from the definition of the elementary representative scale L.

Two asymptotic situations when surfaces are either far from or close to each other are specifically considered in order to shed some light on the numerical results. These two limits allow one to perform some analytical analysis. In the first regime, the macroscopic mean aperture H is considered to be large compared to the composite roughness σ. Their ratio being a small parameter, it is used to expand the flow-factor expressions. In the second regime, it is stated that even if the correlation length λ is smaller than L, it is larger than the minimum aperture. This minimum aperture can be considered as a small parameter to construct a saddle point approximation for flow factors.

The situation when surfaces are far from each other is considered first. This case is related to some weak disorder expansion based on the parameter σ/H, which measures the relative fluctuation of the local aperture field. Expanding relations (7)–(12) in powers of this parameter, one finds, to first order [29], when σ/H is small,

$$\phi_x^y\simeq 1\pm 6\left(\frac{\sigma}{H}\right)^2,\quad \Phi_s\simeq 3\frac{\sigma}{H},\quad \phi_{fp}\simeq 1-3\left(\frac{\sigma}{H}\right)^2, \quad (13)$$

$$\phi_f\simeq 1+\left(\frac{\sigma}{H}\right)^2,\quad \Phi_{fs}\simeq 3\left(\frac{\sigma}{H}\right)^2.$$

This result is generic, and does not depend on the specific characteristics of the microgeometry. Nevertheless, the precise range within which these expressions are valid does depend on the microscopic statistical correlation. In fact, some higher order terms of the weak disorder expansion in the small parameter σ/H are needed to exhibit such a dependence. For example, one needs to consider the third term (the

sixth power of σ/H) to obtain an explicit dependence of ϕ_x on the aperture correlation function [31]. Result (13) show that when surfaces are far from each other, the flow factors tend either to 0 or 1. Then, in this limit, macroscopic equations are perfectly identical to microscopic ones. The aperture heterogeneities do not play any role, and macroscopization is trivial. Relations (13) then give the first correction for macroscopic equations arising from the microgeometry roughness. The physical interpretation of the obtained results can be briefly discussed. The Poiseuille flow factors ϕ_x and ϕ_{fp} are diminished proportionally to the surfaces height variance, showing that the fluid flow and the shear stress due to the pressure gradient are slowed down by the presence of roughness. Some additional fluid flow is then generated by this roughness, proportional to the velocity difference between surfaces through the flow factor Φ_s. Finally, the main shear generated by the roughness is of Couette origin, through flow factors ϕ_f and ϕ_{fs}. This shear, while mostly parallel to the surface velocity difference through the flow factor ϕ_f, has a slight misalignment to this kinematic field through ϕ_{fs}. This amounts to a macroscopic expression of the misalignment between the microscopic one-dimensional roughness direction x and the kinematic surface velocity difference direction $\mathbf{U}_2-\mathbf{U}_1$.

Let us now turn to the second regime, where surfaces are close to contact. It is also possible to obtain some analytical estimates of the flow factor behavior in this regime. To this end, it is necessary to consider the aperture probability density function (PDF) $p(a,x)$, which is the probability of finding an aperture a at position x relative to the prescribed minimum at $x=0$, i.e, a conditional PDF $p(a,x)\equiv p(a(x)|a(0)=0)$. The dependence of $p(a,x)$ on the distance x to the minimum is crucial, because the main contribution to flow factors comes from the aperture distribution near contact. Nevertheless, the precise form of this PDF will not significantly influence the flow-factor dependence with the minimum aperture near contact. Defining some minimal distance $\sigma\epsilon$, with $\min_x a(x)=\sigma\epsilon$, allows one to describe the surface closeness, with a nondimensional arbitrary small parameter ϵ. It is then possible to approximate the negative moments of the aperture distribution given by

$$\langle a^{-n}\rangle=\frac{1}{L}\int_0^L dx\int_0^\infty p(a',x)(\epsilon\sigma+a')^{-n}da', \qquad (14)$$

with a saddle point estimate. This estimate is given, provided that the first and second derivatives of $p(a,x)$, with respect to a, at $a=\sigma\epsilon$, are bounded by

$$\langle a^{-n}\rangle\simeq I(\lambda)\sqrt{\frac{2\pi}{n(n+1)}}(\sigma\epsilon)^{-n+1}, \qquad (15)$$

where $I(\lambda)=\int_0^L p(0,x)dx/L$ is a function of the correlation length λ which depends on the probability function at the minimum, which is not precisely known. Approximation (15) holds for $n>1$. When $n=1$, the saddle point approximation is no longer sufficient to capture the diverging behavior. From Eq. (15), we can thus write the flow factor approximation, near contact, as

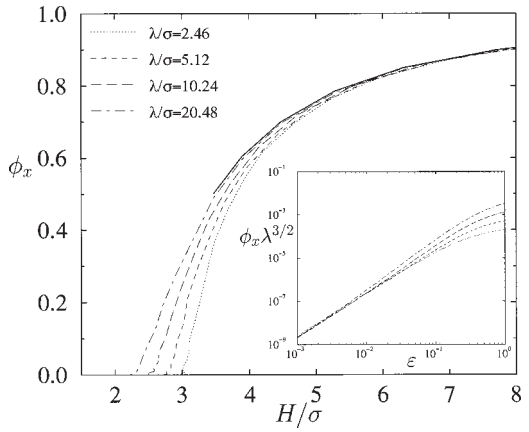

FIG. 4. ϕ_x flow factor for a finite correlation length λ. The continuous line represents the weak disorder approximation expressed in Eq. (13)

$$\phi_x\simeq\sqrt{\frac{6}{\pi}}\frac{\sigma^3}{H_m^3}\ I(\lambda)\epsilon^2,\quad \Phi_s\simeq\frac{H_m}{\sigma}-\sqrt{2}\epsilon,\quad \phi_{fp}\simeq\frac{\sqrt{2}}{H_m}\epsilon. \qquad (16)$$

These results are typical of stochastic geometries. It is expected that flow factors ϕ_x and ϕ_{fp} cancel out when microgeometry surfaces tend toward contact. As a matter of fact, these Poiseuille flow factors, describing the flux and shear induced by the pressure gradient in the direction of streaks, are zero when the passage is blocked up. The precise dependence of these flow factors on the surface minimal distance $\sigma\epsilon$ is governed by the aperture geometry near its minimum. They differ from previous analytical results on deterministic sinusoidal surfaces [32]. For example, ϕ_x displays a power of $\epsilon^{5/2}$ rather than ϵ^2 for a deterministic sinusoidal aperture. Once again, it can be shown that this is a direct consequence of the geometry of the minimum aperture vicinity.

Results (13) and (16) are compared with the numerical computations sketched in Figs. 4–8. These simulations have been performed with a Gaussian short-range-correlation function of the form $C(u)=\sigma^2(1-e^{-u^2/2\lambda^2})$, varying the correlation length λ, by an order of magnitude from

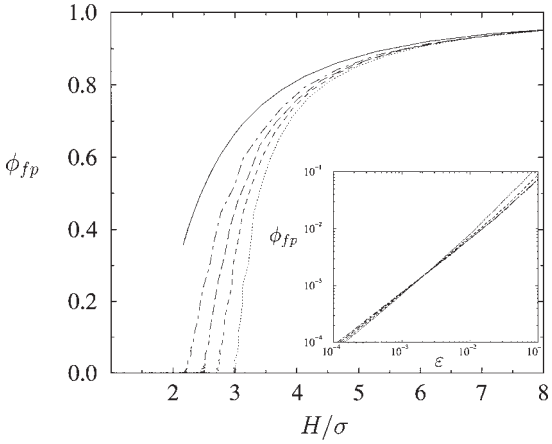

FIG. 5. ϕ_{fp} flow factor for a finite correlation length λ with the same convention as in Fig. 4.

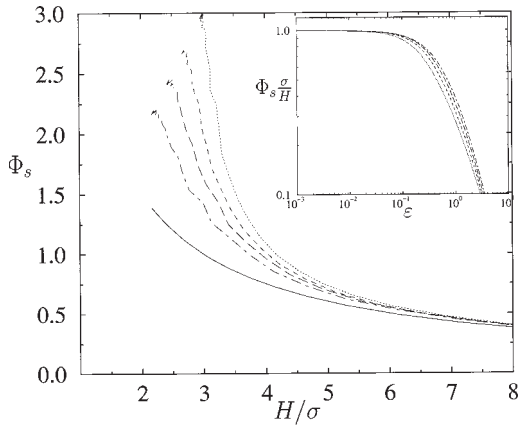

FIG. 6. Φ_s flow factor for a finite correlation length λ with the same convention as in Fig. 4.

$5\times10^{-3}L$ to $5\times10^{-2}L$, for various elementary representative scales L. The flow-factor behavior have shown no dependence on scale L, as expected from flow factors definition and short-range correlation, where $\lambda \ll L$. The insets of the figures especially illustrate Eq. (16) asymptotic behavior. The first estimate [Eq. (13)] is rather good when $H/\sigma > 5$. The saddle point approximation's quality depends on the considered flow factor. The more peaked they are near contact, the better approximated they are. Hence the nondimensional permeability ϕ_x is well captured by the asymptotic due to its -3 power dependence on the local aperture as represented in Fig. 4. Moreover, the ϕ_x prefactor $I(\lambda)$ dependence on λ, has been found from a data collapse of the numerical simulations, indicating a scaling $I(\lambda) \propto \lambda^{-3/2}$. ϕ_{fp} and Φ_s are well described in the close vicinity of contacts by the saddle point estimate, but poorly approximated when $\epsilon > 0.1$.

The analysis of the Couette shear flow factors ϕ_f and Φ_{fs} behavior, in the vicinity of contact shows an algebraic divergence, as sketched in the inserts of Figs. 7 and 8. This divergence is characterized by a power law exponent m :

$$\phi_f \propto \Phi_{fs} \propto (\sigma\epsilon)^{-m}. \tag{17}$$

This algebraic divergence of the shear Couette flow factors, with a minimum distance $\sigma\epsilon$, is qualitatively consistent with

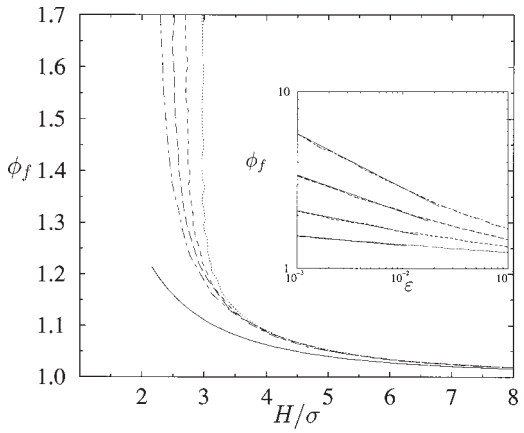

FIG. 7. ϕ_f flow factor for a finite correlation length λ with the same convention as in Fig. 4.

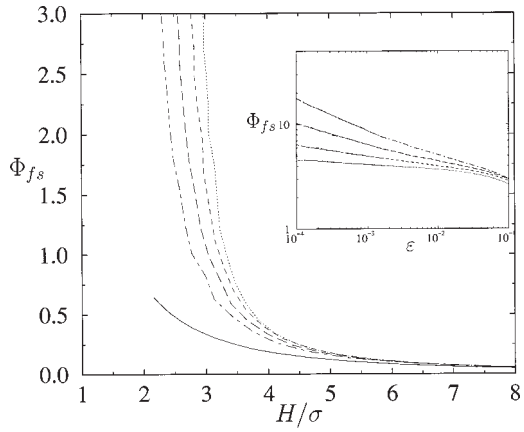

FIG. 8. Φ_{fs} flow factor for a finite correlation length λ with the same convention as in Fig. 4.

the one obtained in the deterministic sinusoidal case [32]. This divergence is associated with an increasing Couette shear, experienced when surfaces are close to contact. However, the power law exponent m depends on the correlation length λ, as can be deduced from Figs. 7 and 8. The larger the correlation length, the more flow factors diverge, and the larger the m exponent is. Nevertheless this dependence is rather smooth, as obtained from Fig. 9, which exhibits a logarithmic dependence: $m \propto -\ln\lambda$. It is noteworthy that when λ is small, the m exponent tends toward zero. The Couette shear divergence disappears as the correlation length tends toward zero. Nevertheless this limit has to be consistently considered with the hypothesis of a small slope, which gives a lower bound for the correlation length $\lambda > \sigma$. In this limit, the divergence of shear Couette flow factors is still algebraic but with a small exponent. The other limit, where $\lambda \simeq L$, extrapolating the results of Fig. 9, gives a value that is close to 1/2, for the exponent m. This value is then consistent with the exponent $m = 1/2$, obtained when analytically computing these flow factors, using a sinusoidal aperture distribution, which coincides with a random aperture profile with correlation length equal to the representative scale L [32].

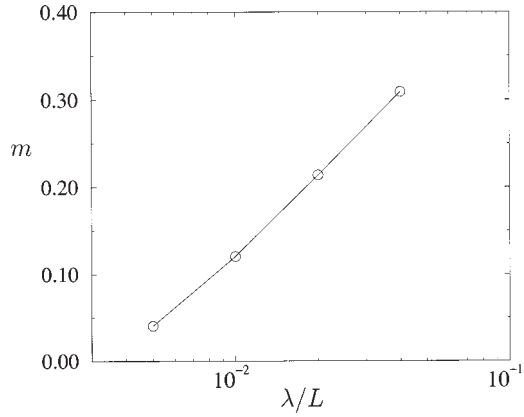

FIG. 9. Power-law coefficient m of the shear Couette flow factor vs the correlation length λ with the same convention as in Fig. 4. The dot size represents the error bars of the numerical computations.

B. Long-range-correlated surfaces

Long-range-correlated self-affine profiles are now under study. Such fractional Brownian motions do not display any typical correlation length, between a lower cutoff ℓ_c and an upper cutoff L_c. The flow factors are nevertheless strongly influenced by their long-range-correlation characterized by the Hurst exponent ζ and the roughness amplitude A.

When surfaces are far apart from each other, the weak disordered results [Eq. (13)] do apply, and give a correct estimate of their dependence on the imposed mean macroscopic distance H. Conversely, when surfaces are close to contact, the transport properties become sensitive to the correlation specificity, in particular in the region where the aperture is minimal. As a matter of fact, fractional Brownian motion displays some interesting specific properties near the maxima and minima. Some results, conjectured from numerical simulations [33], have stated that there are two regimes for the conditional probability density function of the aperture $p(a,x)$ estimated at distance x from the minimum :

$$p(a,x)=\begin{cases}\dfrac{1}{a}\phi\left(\dfrac{a}{x^{\zeta}}\right) & a\gg a^{\star}\\ \propto x^{-1-\zeta} & a\ll a^{\star},\end{cases} \tag{18}$$

Here $a^{\star}(x^{\star})$ is the typical aperture for which the fractional Brownian motion loses the memory of the maximum (or minimum) position far from $x^{\star}$. These two constants are related by the affinity scaling $a^{\star}=Ax^{\star\zeta}$. The first regime of Eq. (18) is simply given by the rescaling invariance of the aperture cumulative distribution function. The second regime is far from simple and there is, for now, no mathematical demonstration of it [34]. This twofold behavior is nevertheless known in the special case of Brownian motion when $\zeta=1/2$. The specific behavior of the aperture field near contact influences flow factors when surfaces are near contact. The normalization condition of the PDF is related to the upper and lower cutoffs L_c and ℓ_c:

$$\int_{\ell_c}^{L_c}dx\int_0^{\infty}p(a,x)da=1. \tag{19}$$

The representative typical scale L for averaging flow factors has to be chosen so that $L\geqslant L_c$. For the sake of simplicity, one has chosen $L=L_c$ in the following, while other choices would nevertheless not have modified the obtained results. As previously done, a saddle point estimate of the negative moment of the aperture can be computed, from the definition

$$\langle a^{-n}\rangle=\frac{1}{L_c}\int_{\ell_c}^{L_c}dx\int_0^{\infty}da'p(a',x)(\epsilon\sigma+a')^{-n}da. \tag{20}$$

Taking relation (18) into account, it can be approximated, for a small ϵ,

$$\langle a^{-n}\rangle\simeq\frac{1}{L_c}\int_{\ell_c}^{x^{\star}}dxx^{-1-\zeta}\sqrt{\frac{2\pi}{n(n+1)}}(\sigma\epsilon)^{-n+1}. \tag{21}$$

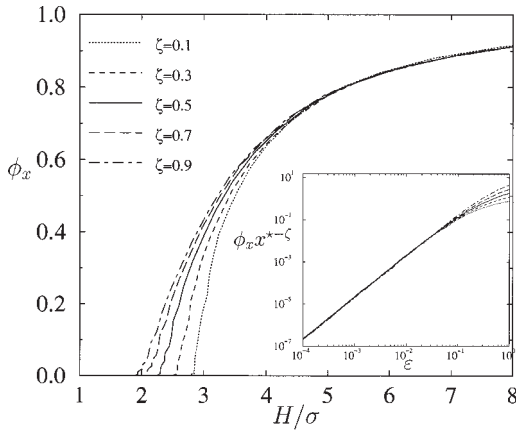

FIG. 10. ϕ_x for a self-affine aperture. Hurst exponents ranging from 0.1 to 0.9 have been computed. The inset shows the numerical data collapse obtained using rescaling [Eq. (24)] near the contact.

Using normalization (19), one can estimate in the limit, where $x^{\star}\ll L_c$,

$$\int_{\ell_c}^{x^{\star}}dxx^{-1-\zeta}a^{\star}\simeq 1-\int_1^{\infty}u\,\phi(u)du. \tag{22}$$

The right-hand side of relation (22) is constant; then, near contact, the simple result holds:

$$\langle a^{-n}\rangle\propto\frac{1}{x^{\star\zeta}L_c\sqrt{n(n+1)}}(\sigma\epsilon)^{-n+1}. \tag{23}$$

From this estimate, one can compute the flow factors' asymptotic expressions near contact :

$$\phi_x\propto\frac{\sigma^2x^{\star\zeta}}{H_m^3}L_c\epsilon^2,\quad \phi_s\simeq\frac{H_m}{\sigma}-\sqrt{2}\epsilon,\quad \phi_{fpx}\simeq\frac{\sqrt{2}}{H_m}\epsilon. \tag{24}$$

One may note that these asymptotic behaviors are quite close to the previous results for finite correlation length [Eq. (16)]. Their dependence on the minimum distance ϵ is identical, but the prefactor of ϕ_x now displays some dependence on the Hurst exponent ζ and the upper cut off L_c. It is interesting to note that an increasing correlation of the aperture, associated with an increasing Hurst exponent, leads to an increasing permeability when surfaces are close to contact.

These estimates are fully consistent with numerical results reported in Figs 10–12. Scaling (24) allows a data collapse of every numerical computation of the nondimensional permeability ϕ_x near contact when the Hurst exponent varies. The linear dependence of ϕ_x, with upper cutoff L_c, has also been numerically checked, but is not represented in these figures for clarity's sake. Simulations sketched in Figs. 10–12 also permit one to estimate the validity of the saddle point approximation [Eq. (24)], which begins to hold when $\epsilon<0.1$.

As previously observed, Couette shear flow factors ϕ_f and Φ_{fs} diverge when surfaces are close to contact. From the twofold aperture behavior near contact [Eq. (18)], it is clear

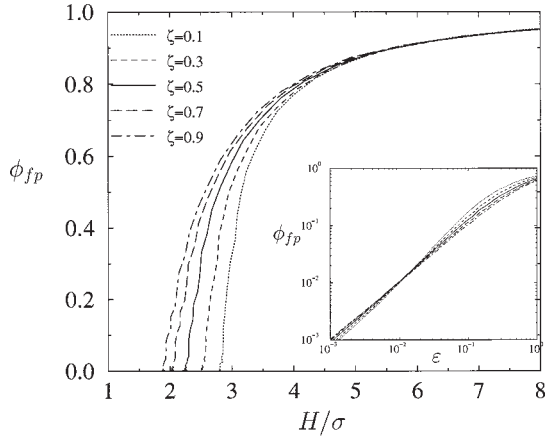

FIG. 11. ϕ_{fp} for a self-affine aperture with the same conventions as in Fig. 10.

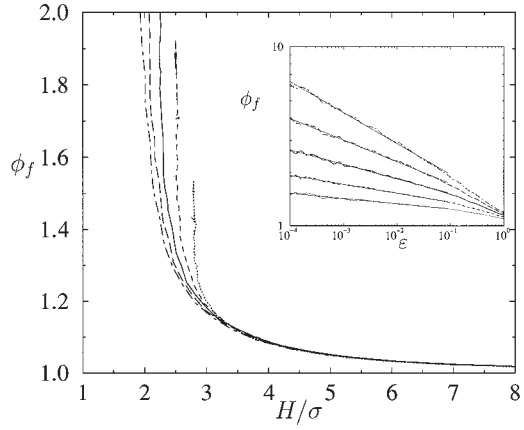

FIG. 13. ϕ_f for a self-affine aperture with the same conventions as in Fig. 10. The inset shows a power-law divergence that depends on the Hurst exponent near contact.

that their shared divergence with the $\langle a^{-1}\rangle$ moment cannot be captured by a rough saddle point estimate. This divergence numerically display the same interesting power law behavior as in the previous section. More precisely, the insets of Figs. 13 and 14 show the power law behavior near contact, whose exponent m depends on the Hurst exponent ζ. The more correlated the aperture field is, the higher the value of ζ is and more divergent the Couette shear is. This joint behavior can be related to the Hurst exponent, as sketched in Fig. 15. This figure displays a power law dependence of shear flow factors near contact, which have the form

$$\phi_f \propto \Phi_{fs} \propto \epsilon^{-m} \propto \epsilon^{-(dc^{\zeta})}, \tag{25}$$

where c and d are two constants related to the surfaces amplitude A. Such an algebraic divergence of the Couette shear flow factors was already obtained for a finite correlated aperture. Here the power law exponent m of this algebraic divergence is shown to depend algebraically on the Hurst exponent. The power law exponent m can be extrapolated from Fig. 15 for Hurst exponent values $\zeta \to 0$ and $\zeta \to 1$, for which it exhibits the extreme values $m \to 0$ and $m \to 0.25$. These limits are consistent with the ones previously obtained for finite correlation in Sec. II. $\zeta \to 0$ is associated with a decorrelation of the aperture field, where the algebraic divergence of the Couette shear flow factors disappears. The $m \simeq 0.25$ value obtained in the other limit, where $\zeta \to 1$ is bounded as expected by the deterministic result on a sinusoidal aperture, for which $m = 1/2$.

These results show that the Couette shear stress is strongly influenced by the long-range nature of the aperture field, especially near contact. Numerically, the Couette shear stress displays a power law dependence with the Hurst exponent, which cannot be captured by a saddle point approximation. It is nevertheless tempting to associate the algebraic dependence of the power law exponent m with the specific behavior of fractional Brownian motion near contact.

IV. CONCLUSIONS

Newtonian lubricant flow, between two microscopically statistically independent anisotropic surfaces in sliding motion without solid contact, has been studied. The macroscopic flux and shear experienced by both surfaces are related to their microscopic roughness through five nondimensional flow factors. The aperture field between surfaces entirely determines these flow factors. They have been

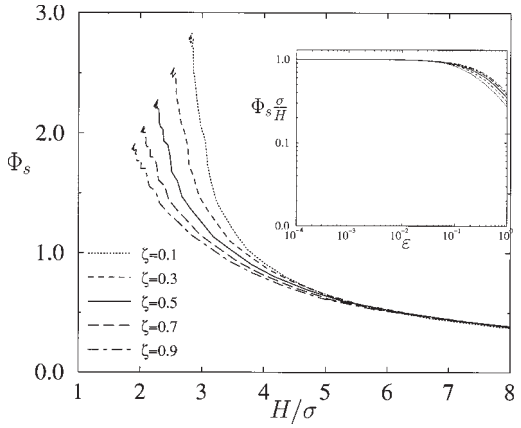

FIG. 12. Φ_s Flow factor for a self-affine aperture with the same conventions as in Fig. 10.

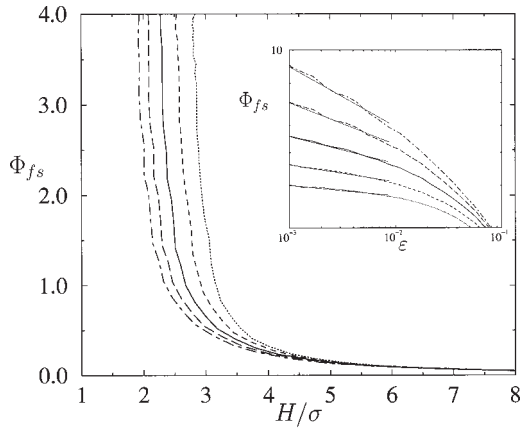

FIG. 14. Φ_{fs} for a self-affine aperture with the same conventions as in Fig. 13.

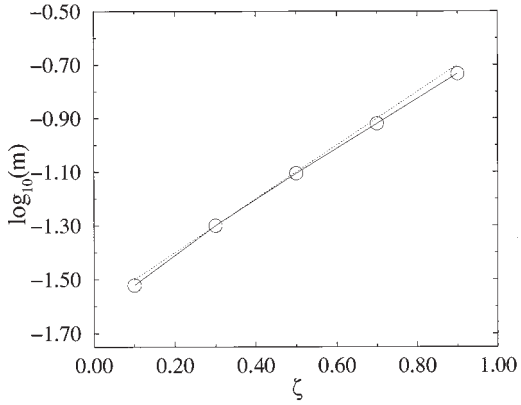

FIG. 15. Diverging Couette shear flow factors exponent m near contact, vs the Hurst exponent ζ. The dot size represents the error bars of the numerical computations.

computed numerically for short- and long-range aperture correlations. Asymptotic situations, where surfaces are either close to one another or far apart, have been analytically studied and compared to numerical calculus. The Poiseuille flow factors ϕ_x and ϕ_{fp}, and the Couette shear flow factor Φ_s, exhibit rather generic behaviors when surfaces are close to contact. It has nevertheless been found that the nondimensional permeability ϕ_x prefactor does depends on the aperture correlation. Couette shear flow factors ϕ_f and Φ_{fs} diverge as surfaces are brought into contact. The exact nature of this divergence depends strongly on the aperture correlation. For a short-range-correlated profile, the Couette shear flow factors diverges algebraically, with a power law exponent which logarithmically depends on the correlation length. For a long-range-correlated profile, the Couette shear flow factor exhibits an algebraic divergence with the minimum aperture. It has been found numerically that this divergence has a power law dependence on the Hurst exponent of the aperture correlation.

This study has been confined to uncorrelated profiles. Some of the obtained results are modified when the top and bottom surfaces are intercorrelated. Such a correlation between solid surfaces occurs naturally during the rolling process, where roughness is transferred from the steel roll to the workpiece [12] as well as in any process where deformations conform the two pieces one another. In this case, one has to consider a spatiotemporal average rather than a simple spatial average in order to compute flow factors, as indicated in Ref. [36]. For a simple deterministic geometry, analytical results show that intercorrelation mainly affects ϕ_s and ϕ_{fs} [32], which are equal to zero when top and bottom profiles are identical. Moreover, numerical simulations as well as symmetry considerations indicate that this result also apply for random identical profiles [35].

Moreover, the obtained result for the shear flow factors strongly depends on the one dimensional confinement of the microgeometry. In particular, the divergence of the shear Couette flow factors will be smoothed out by two-dimensional effects. In the case of a two-dimensional microscopic roughness, flow factors cannot be computed directly from the moments of the local aperture, but must be evaluated from two-dimensional numerical computations required to solve closure problems [36]. Such a procedure should exhibit, at some point, nondiverging shear flow factors when reaching solid contact between surfaces. Finally, some nondimensional coefficients, characterizing the anisotropy of the microscale roughness —such as the Peklenik number found in Refs. [26,4]— should provide a natural lower cutoff for the reported diverging behaviors.

ACKNOWLEDGMENTS

We would like to thank R. Cerf, P. Carmona, and S. Roux for interesting discussions. This work was supported by the Research Project Contract (CPR) ‘‘Mise en forme des matériaux: Contact outil-métal-lubrifiant’’ between CNRS (SCa), Irsid (Usinor Group), Péchiney Center de Recherche de Voreppe, Paris Sud Orsay University (LMS), Collège de France (PMC), ECL (LTDS), INPT (IMFT), INSA de Lyon (LMC), and ENSMP (CEMEF).

[1] W. Li, C.I. Weng, and C. Hwang, Tribol. Trans. **40**, 111 (1997).
[2] P. Goglia, T. Conry, and C. Cusano, J. Tribol. **106**, 104 (1984).
[3] N. Patir and H. Cheng, J. Lubr. Technol. **100**, 12 (1978).
[4] N. Patir and H. Cheng, J. Lubr. Technol. **101**, 220 (1979).
[5] B. Bhushan and G. Blackman, ASME J. Tribol. **113**, 452 (1991).
[6] L. He and J. Zhu, Wear **208**, 17 (1997).
[7] G. Zhou, M.C. Leu, and D. Blackmore, Wear **170**, 1 (1993).
[8] J. Gagnepain and C. Roques-Carmes, Wear **109**, 119 (1986).
[9] E. Doege, B. Laackman, and B. Kischnik, Metal Working **66**, 113 (1995).
[10] A. Mahumdar and C.L. Tien, Wear **160**, 313 (1990).
[11] M. Yang and F. Talke, Wear **170**, 15 (1993).
[12] F. Plouraboué and M. Boehm, Tribol. Int. **32**, 45 (1999).
[13] S. Suryaprahash and B. Bhushan, Wear **180**, 17 (1995).
[14] P. Adler and J. Thovert, *Fractures and Fracture Network* (Kluwer Academic Publishers, Amsterdam, 1999).
[15] F. Plouraboué *et al.*, Phys. Rev. E **51**, 1675 (1995).
[16] V. Mourzenko, J. Thovert, and P.M. Adler, Phys. Rev. E **53**, 5606 (1996).
[17] S.R. Brown, J. Geophys. Res. **92**, 1337 (1987).
[18] S.R. Brown, S. Chen, and J.D. Sterling, J. Geophys. Res. **94**, 9429 (1989).
[19] V. Mourzenko, O. Galamay, J. Thovert, and P.M. Adler, Phys. Rev. E **56**, 3167 (1997).
[20] F. Plouraboué, P. Kurowski, J.M. Boffa, J.P. Hulin, and S. Roux, J. Contam. Hydrol. **46**, 295-318 (2000).
[21] F. Plouraboué, J.P. Hulin, S. Roux, and J. Koplik, Phys. Rev. E **58**, 1 (1998).
[22] J. Schmittbuhl, J.P. Vilottte, and S. Roux, Physica A **26**, 6115 (1993).

[23] V. Mourzenko, J. Thovert, and P.M. Adler, Phys. Rev. E **59**, 4265 (1999).
[24] H. Auradou *et al.*, Phys. Rev. E **60**, 7224 (1999).
[25] N. Phan-Thien, Proc. R. Soc. London, Ser. A **374**, 569 (1981).
[26] H. Christensen and K. Tonder, J. Lubr. T. **93**, 324 (1973).
[27] L. Chow and H. Cheng, J. Lubr. Technol. **98**, 117 (1976).
[28] G. Bayada and M. Chambat, J. Tribol. **110**, 402 (1988).
[29] J. Tripp, J. Lubr. Technol. **105**, 458 (1983).
[30] H.A. Makse, S. Havlin, M. Schwartz, and H.E. Stanley, Phys. Rev. E **53**, 5445 (1996).
[31] A. Dewitt, Phys. Fluids **7**, 2553 (1995).
[32] N. Letalleur, F. Plouraboue, and M. Prat (unpublished).
[33] F. Plouraboué, S. Roux, J. Schmittbuhl, and J.P. Vilotte, Fractals **3**, 113 (1995).
[34] Pr. Philippe Carmona (private communication).
[35] N. Letalleur, Ph.D. thesis, INSA Lyon, 2000.
[36] M. Prat, F. Plouraboue, and N. Letalleur, Transp. Porous Media (to be published).